Hassan Md Sahid (Orcid ID: 0000-0003-0466-5395)

Low-Temperature Selective Laser Sintering 3D Printing of PEEK-Nylon Blends: Impact of Thermal Post-Processing on Mechanical Properties and Thermal Stability

Luis A. Chavez[1,2], Paulina Ibave[1,2], Md Sahid Hassan[1,2], Samuel E. Hall-Sanchez[1,2], Kazi Md Masum Billah[1,2], Alba Leyva[1,2], Cory Marquez[1,2], David Espalin[1,2], Sabrina Torres[3], Thomas Robison[3], Yirong Lin[1,2,*]

[1]Department of Mechanical Engineering, The University of Texas at El Paso, El Paso, TX 79968, USA

[2]W.M. Keck Center for 3D Innovation, The University of Texas at El Paso, El Paso, TX 79968, USA

[3]National Security Campus operated by Honeywell 14520 Botts Rd., Kansas City, MO 64147, USA

*Corresponding author. *Email address:* ylin3@utep.edu

Abstract

A high-performance polymer (Polyether ether ketone, PEEK) blended with a commercial low-temperature polymer (Polyamide 12, PA-12) was fabricated using a low-temperature selective laser sintering 3D printer. Different post-processing heat treatments were implemented after fabrication to tune the thermal and mechanical properties of printed blends. The specific mechanical modulus of the blend was increased up to 79% in comparison to printed PA-12 samples with heat treatment. Additionally, the thermal resistance of the treated blends greatly exceeded the properties observed using PA-12 alone. This research proposes a methodology to fabricate and engineer high-performance polymers using desktop SLS printers through a secondary lower melting temperature material and heat treatments.

Introduction

Since its initial commercialization, additive manufacturing (AM) has become a must-have tool in multiple emerging and legacy industries. AM, or 3D printing, is a technology in which complex geometries are built in a layer-by-layer fashion. Although initially utilized as a rapid prototyping tool, AM has steadily gained attention as a technology that could use to fabricate functional end-product components due to its reduced times of fabrication, as well as the geometry design freedom that it provides [1-3]. However, AM has not yet been fully implemented as a mass-manufacturing tool in many industries due to two main drawbacks that go hand-in-hand: material selection and manufacturing equipment capabilities [4,5].

AM equipment can be generally classified in two categories: "desktop" printers and industrial/research grade machines. While AM desktop printers are now readily available and easy to use, they are designed for manufacturing materials with properties below the industrial standard [6]. The materials conventionally printed using desktop printers are polymers with low melting points and mechanical properties not generally suitable for structural applications. This is partially due to the temperature limitations observed in conventional desktop printers, which operating at temperatures below 300 ℃ [4]. However, high-performance materials usually require processing conditions above this temperature. AM machines that can manufacture high-performance materials such as ceramics and metals are currently available [7], yet they are prohibitively expensive to acquire and operate in many low-cost settings.

High-performance polymers (HPP) are a material class that aims to alleviate current manufacturing limitations by providing mechanical properties similar to those observed in metals and ceramics but at much lower processing temperatures and cost [8]. One of the most prominent HPP groups is the PAEK (Polyaryletherketone) family [9]. PAEK is a family of semi-crystalline thermoplastics with high-temperature stability and mechanical strength, suitable for materials required to sustain variable environments, and thus crucial in industrial and medical applications [10,11]. Among the PAEK family,

This is the author manuscript accepted for publication and has undergone full peer review but has not been through the copyediting, typesetting, pagination and proofreading process, which may lead to differences between this version and the Version of Record. Please cite this article as doi: 10.1002/app.52290

one of the most prominent members is PEEK (Polyether ether ketone). PEEK can be used for load-bearing applications due to its remarkably high strength (240 MPa), impact resistance, and fatigue resilience [12]. The molecular structure in PEEK is a linear chain of hundreds of monomer units with a remarkably high molecular weight and chain length that ranges from 20,000-120,000 g/mol [13,14]. PEEK's molecular properties are characteristic of superior impact resistance and polymer bond strength due to increased entanglement of the polymer chains.

Additionally, the length and composition of the molecular chain result in unique attributes in the polymer, most notably its thermal resistance at temperatures exceeding 200 °C and high dimensional stability due to low moisture absorption [15]. Furthermore, the chemical structure of PEEK exhibits resistance to chemical and radiation damage, compatibility with many reinforcing additives (such as glass and carbon fiber), and superior strength compared to some low-cost tooling metals [16]. PEEK has also been demonstrated to be highly compatible for biomedical applications, including prosthetics, porous scaffold, and replacement bone, and has been posed as a great candidate to replace metals in the bio-implant industry [10–12].

While PEEK properties rival those found in metals for several applications [17], most of its manufacturing is still being done through conventional techniques [11,16]. The processing temperatures required to manufacture PEEK above what typical desktop printers can achieve. Injection molding of PEEK typically requires barrel and nozzle temperatures in the region of 400 °C [18]. In addition to these high-temperature requirements, PEEK components also need to have uniform temperature distributions to achieve consistent properties. Due to these thermal processing limitations, PEEK components are fabricated using special tooling and molding, currently inhibiting their implementation into applications where custom dimensions and shapes are required [19]. Although the high thermal and mechanical performance of PEEK have made it highly attractive, some of these inherent properties have limited its manufacturability through AM technologies.

Recently PEEK fabrication has demonstrated progress in using AM machines; this has only been done using industrial-grade equipment that can operate at the high temperatures required for PEEK processing. This leads to similar limitations to those observed in the AM of metals and ceramics [20]. There is an industrial and research need to develop methods for PEEK components to be fabricated using low-power desktop low-cost 3D printing solutions. In this work, we have studied the feasibility of fabrication through Selective Laser Sintering (SLS) AM of a PEEK–Polyamide-12 (PA-12, Nylon) blend using a low-power SLS printer (Sinterit LISA). The PA-12 was employed as a binder to PEEK powder in the SLS process. A custom post heat-treatment method was employed to improve the mechanical and thermal properties of this blend. Ideal heat treatment conditions were determined, and the ability to 3D print high-performance polymers using low-power equipment was demonstrated.

Methods

Materials

Laser light from diode laser source is reflected instead of being absorbed by the powder [21] during printing process. To increase the laser absorbability of powder, carbon-coated PA-12 powder (average particle size of 50 μm, Sinterit) was blended with PEEK powder (average particle size of 75 μm, Polyclean Technologies). The two powders were mechanically mixed in a PEEK: PA-12 at a 70:30 volume ratio to create the printing feedstock.

Fabrication process

The newly prepared feedstock was used to manufacture Type V tensile specimens with dimensions described in ASTM D-638. The orientation of the specimen during the printing process is shown in Figure 1. In order to reduce overhang and part dragging during fabrication, a sacrificial base was added and attached to the tensile specimens using cylindrical pillars with a diameter and height of 2mm. The fabricated structures were detached from the sacrificial base using a sharp blade. The tensile specimens were fabricated using a Sinterit LISA SLS 3D printer, and the utilized printing parameters are shown in Table 1. It is important to note that this machine has a maximum chamber temperature of 190 ℃ and a laser power of 5W. A Laser Power Multiplier parameter was utilized to increase the time spent by the laser in a single point. Those parameters are selected to output maximum energy density considering the high melting temperature of PEEK.

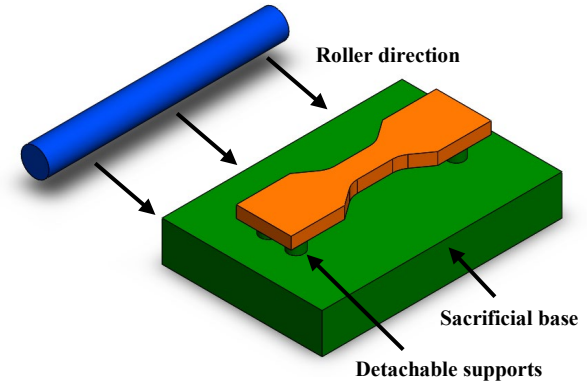

Figure 1. Schematic of printing model and orientation during fabrication.

Table 1. Utilized printing parameters for the PEEK:PA-12 mixture.

Parameter	Value
Laser Power (W)	5
Laser Power Multiplier	2.5
Scan Speed (mm/s)	500
Layer Thickness (mm)	0.125
Chamber Temperature (℃)	180
Z Shrinkage (%)	90
Hatch Distance (mm)	0.36
Energy Density (J/mm^3)	0.222

Post-processing

In order to overcome the previously discussed manufacturing limitations, PEEK-PA12 composites were initially fabricated then post-processed to obtain a pure PEEK part. PA-12 would first act as a printing aid and become the matrix for PEEK particles, as shown in the first stage of Figure 2. Once composites were printed, a heat-treatment process was introduced to use PA-12 as a liquid phase sintering aid. This liquid phase sintering step occurs during stage two, shown in Figure 2, allowing for PEEK particles to rearrange as PA-12 melts due to exposure to high temperatures. During the third stage of the heat-treatment process, only PEEK particles remain, interparticle mass diffusion and densification of the component is promoted through prolonged exposure to high temperatures. Finally, the component is cooled down and retrieved.

Three tensile specimens were randomly selected and placed in a boron nitride powder bed inside an alumina crucible for uniform heating throughout printed coupons. The crucible was then subjected to an atmospheric pressure in air and different sintering profiles determined by the design of experiments. A sintering temperature of 365 ℃ was used for all profiles. Atmosphere and sintering temperature remained consistent to ensure PA-12 degradation, which was determined through preliminary thermogravimetric studies. A Taguchi design of experiment was implemented to determine ideal heat-treatment parameters for this polymer blend. The parameters studied for this purpose were heating rate (HR), sintering time (ST), and cooling rate (CR). HR and CR dictate the material and mechanical properties of thermally treated PEEK samples [22,23]. The HR stage was expected to influence sintering uniformity throughout the samples and sintered density of samples, as well as sintering temperature of PEEK. Meanwhile, CR was expected to influence the crystallinity and therefore the mechanical properties of the PEEK-containing components. ST was expected to have an influence on PA12 residual concentration and sintered density. Table 2 shows the different parameter levels used of each of these parameters.

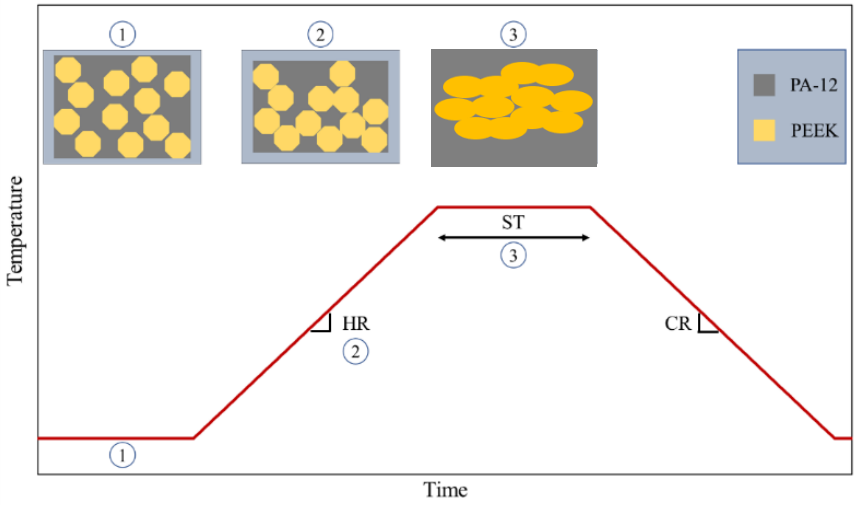

Figure 2. Schematic of sintering profile and geometrical evolution of the fabricated parts during this sintering process.

Table 2. Sintering profiles utilized for this study.

Sintering Profile	Sintering Time (ST) [min]	Heating Rate (HR) [℃/min]	Cooling Rate (CR) [℃/min]
111	1	1	1
122	1	10	10
211	60	1	1
222	60	10	10
312	120	1	10
321	120	10	1
412	960	1	10
421	960	10	1
Green Body (GB)	Samples tested as printed, no heat treatment performed.		

Here, 1st digit of Sintering profile indicates ST (1st digit value: 1=1min, 2=60min, 3= 120min, 4= 960min)

2nd digit of Sintering profile indicates HR (2nd digit value: 1=1^{0}C/min, 2=10^{0}C/min)

3rd digit of Sintering profile indicates CR (3rd digit value: 1=1^{0}C/min, 2=10^{0}C/min)

Characterization

Mechanical characterization was performed using an INSTRON 5866 load frame, a non-contacting video extensometer, and a modified ASTM D-638 procedure. The specimens were tested at a displacement rate of 0.1mm/min instead of the standard 1mm/min to accommodate the samples' shrinkage due to heat treatment. Thermogravimetric analysis (TGA) was carried out using TGA-55 from TA Instruments. TGA characterization was performed by heating samples up to 700 °C at a 10 °C/min rate in an air atmosphere. Finally, the morphology of the specimens after heat treatment was characterized using Field Emission Scanning Electron Microscope S-4800 from Hitachi High-Tech America Inc. In order to obtain high resolution images, gold sputtering was performed before performing SEM characterization. A conductive layer of metal using gold on the sample through gold sputtering was generated that inhibits charging, reduces thermal damage, and improves the secondary electron signal that is required for topographic examination in the SEM. 108 Auto/Se sputter coater (TED PELLA, Inc, CA, USA) was used to perform gold sputtering. For gold sputtering 0.3psi nitrogen flow was confirmed, and 10micron of gold-sputtered thickness was deposited on SEM samples.

Results and Discussion

The density of the different samples was obtained by measuring the weight and external volume of the samples after their respective heat treatment processes were performed. These densities are shown in Figure 3. A density of 0.9 g/cm^3 was obtained for the untreated PA-12 sample using the previously described printing parameters. In contrast, the untreated PEEK/PA-12 polymer blend (Green Body) samples exhibited a marked decrease in density at 0.58 g/cm^3. This is an indication that although the theoretical density of PEEK is higher than that of PA-12, PEEK particles were not sintered during the printing process due to the temperature and power limitations of the 3D printer. However, once heat treatment postprocessing was introduced, higher densities were achieved. During this thermal post-processing the PA-12 inside of the samples melted, allowing for a geometrical reorganization of the PEEK particles, decreasing the volume of the parts and increasing its density. In addition to this geometrical reorganization, PEEK particles are expected to coalesce at the temperatures introduced during the heat treatment. The density of the samples was observed to increase as longer heat treatment conditions were introduced for up to a sintering time of two hours. However, when the specimens were exposed to longer sintering times (16 hours), a decrease in density was observed. This decrease in density contrasted with the samples treated for two hours and is believed to be due to two competing phenomena: while higher densities are expected to be achieved as a result of PEEK particle coalescence under prolonged exposure to temperature, the PA-12 present in the blend samples would simultaneously degrade and evaporate, resulting in increased porosity. Therefore, in terms of density, the ideal heat treatment condition for the prepared polymer blend was 321 (ST 120 minutes, HR 1 °C/min, and CT 10 °C/min).

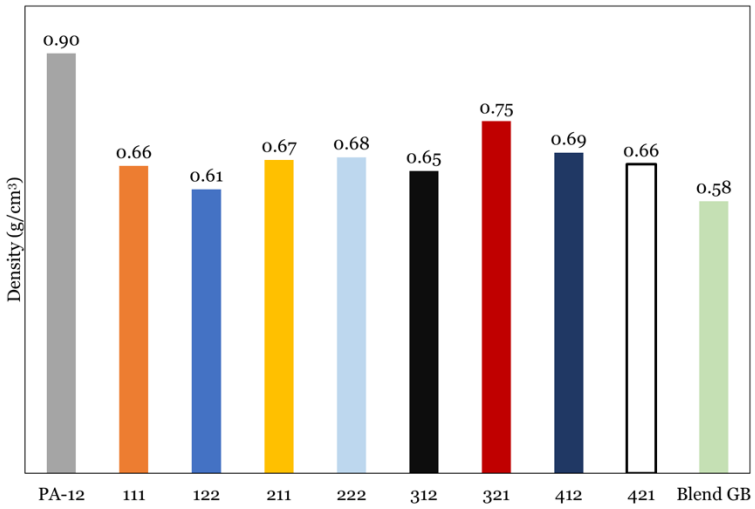

While all samples survived the various heat treatment process and density characterization, not all samples were strong enough to be mechanically characterized. The polymer blend without any heat treatment, as well as the samples with longer heat treatment processes, 412 and 421, exhibited brittle failure at very low loads or while handling. The mechanical properties of the remaining samples were normalized using their densities. A summary of these specific mechanical properties is shown in Figure 4. Untreated PA-12 printed samples exhibited a specific tensile modulus of 0.57 MPa·m^3/kg. As previously stated, the presence of PEEK powder in the polymer blend results in lower densities and mechanical properties to those of untreated PA-12. However, these properties could be recovered or even improved using thermal postprocessing. Notably, the sintering time was found to have a positive effect in mechanical properties as longer times were introduced up to a holding time of two hours. Samples that were held at the sintering temperature for one minute exhibited an average specific modulus of 0.44 MPa·m^3/kg, followed by samples exposed at sintering temperature for one hour at 0.50 MPa·m^3/kg, and by samples held for two hours, which achieved the highest average specific tensile modulus at 0.73 MPa·m^3/kg. Meanwhile, samples exposed to a sintering time of 16 hours were mechanically weak and exhibited a brittle behavior; it is believed to be caused by the burnt-out of PA-12 binder in the sample. The amount of PA-12 remaining in the samples was characterized through thermogravimetric analysis and is shown in Figure 5.

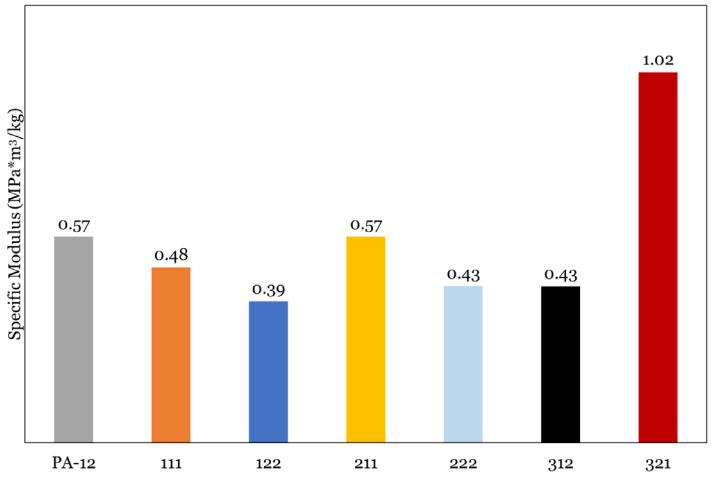

Figure 4. Mechanical properties of fabricated samples under different heat treatment processes.

Based on the TGA data shown in Figure 5, several phenomena can be observed. First, it was noted that the samples subjected to no heat treatment (Blend GB), or to a brief heat treatment (122, 222) exhibited two marked temperature ranges where the considerable mass loss was present. This behavior can be better observed using the slope of this thermogravimetric characteristic, shown in Figure 6. Additionally, these samples with little to no thermal exposure (Blend GB, 122, and 222) exhibited a mass loss peak at a temperature of ℃, as well as a wide peak in the temperature range of 585-625 ℃. The first mass loss peak matched the thermal characteristics of PA-12, while the second, boarder peak is commonly observed in PEEK. Although the heat treatment processes were designed to eliminate PA-12 from the samples, considerable amounts of this material remained in the specimens regardless of sintering time. The remaining PA-12 is expected to have a significant impact on the overall properties of the fabricated polymer blend structures. Therefore, PA-12 content in the various samples was quantitatively determined by heat treatment in air at 425 ℃, given that the degradation shifts from PA-12 to PEEK around this temperature.

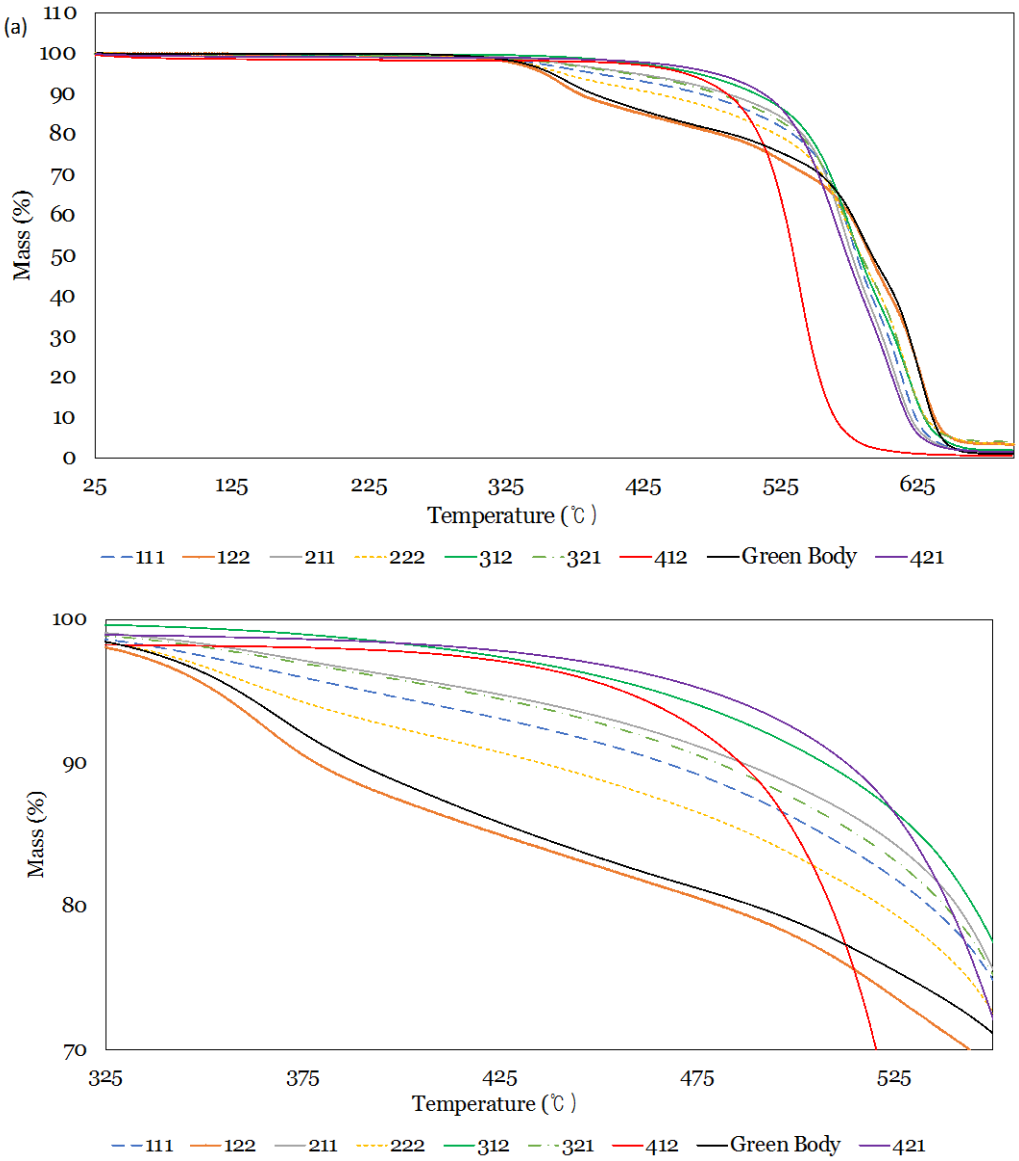

Figure 5. (a) TGA of the polymer blends with different heat treatments (b)1 to 30% weight loss in thermogram.

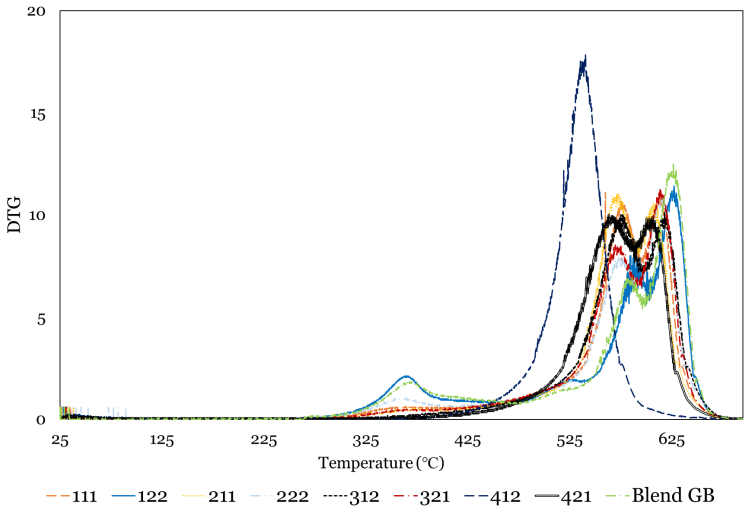

Figure 6. Differential thermogravimetric properties under different heat treatments.

The amount of PA-12 remaining in the different samples is shown in Figure 7 (a). Significant discrepancies between the amount of PA-12 lost during the TGA studies and that in the original blend were observed. The blend without any heat treatment exhibited a PA-12 mass loss of only 13.68% instead of the expected 24.7% from the original 70:30 volume blend ratio. It is believed that polymer blending occurred as a result of higher miscibility obtained in the materials due to the 3D printing process and the heat treatment induced by the TGA experiments [24, 25]. Additionally, PEEK and PA-12 have been shown to have some compatibility [26]. Lower PA-12 concentrations were observed for samples that were heat treated for longer periods, as expected based on the thermal properties of this material. Despite the prolonged exposure to thermal degradation conditions, PA-12 was still present in all polymer blends after heat treatment. Based on thermal and mechanical characterization, it was found that a residual PA-12 concentration of about 5.62 ± 0.77 wt.% was ideal to achieve high mechanical properties based on the sintering profiles that exhibited the highest response. Higher PA-12 concentrations would inhibit a proper mechanical load transfer to PEEK material thus lower PA-12 levels are believed to provide higher specific mechanical properties, which could be achieved through long exposure to heat treatment. However, excessive heat treatment sintering time was also found to degrade the overall thermal properties of PEEK, as shown in Figure 7(b).

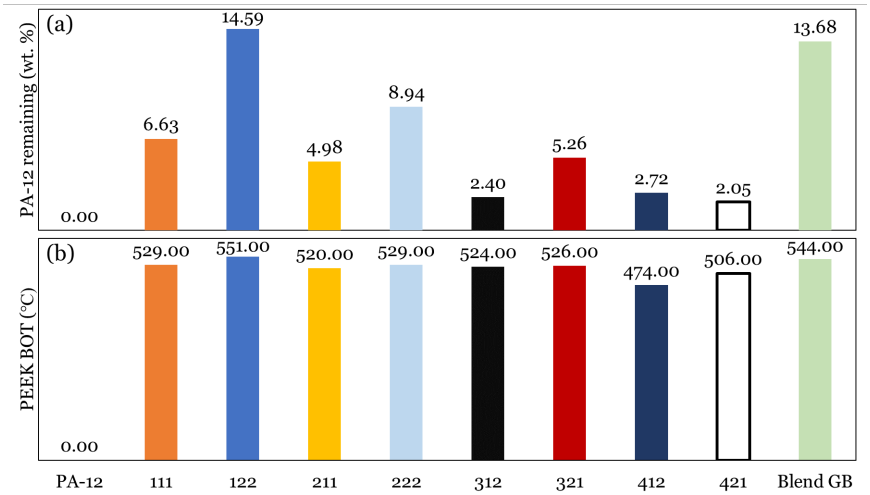

Figure 7. (a) amount of PA-12 remaining in the samples after heat treatment, (b) impact of heat treatment in thermal degradation temperature (burn-out temperature, BOT) of PEEK.

Finally, SEM characterization was performed in an effort to correlate the mechanical and thermal properties with the microstructure of the different material systems. The images of these different samples are shown in Figure 8. An ideal morphology would be similar to that depicted in the pure PA-12 sample, where boundaries between the polymer particles are fused together. Although voids can be observed in the sample, the polymer is interconnected, as shown in Figure 8(a). In contrast, PEEK particles embedded in the PA-12 matrix could be observed in the GB samples, as shown in Figure 8(b). An evolution of the microstructure was observed as a function of the heat treatments in Figure 8(c-i). First, it was seen that the PA-12 matrix melted and wetted the PEEK particles to create a uniform, yet still heterogeneous, polymer composites, as shown in Figure 8 (c-h). It was also seen that the samples with the higher mechanical properties exhibited a better mixing of their components, Figure 8 (e) and (h), where it was more difficult to see the individual particles of PEEK in the PA-12 matrix. Finally, individual PEEK particles could be observed as a result of the decomposition of PA-12 in the samples that were exposed to prolonged heat treatments, as shown in Figure 8 (g) and (i). Based on these results, it is believed that the use of different heat treatments may promote polymer alloying or better miscibility [27,28] of different polymeric materials to create a polymer blend that exhibits the high thermal and mechanical properties of the high-performance engineering polymer and the low-energy manufacturability of PA-12.

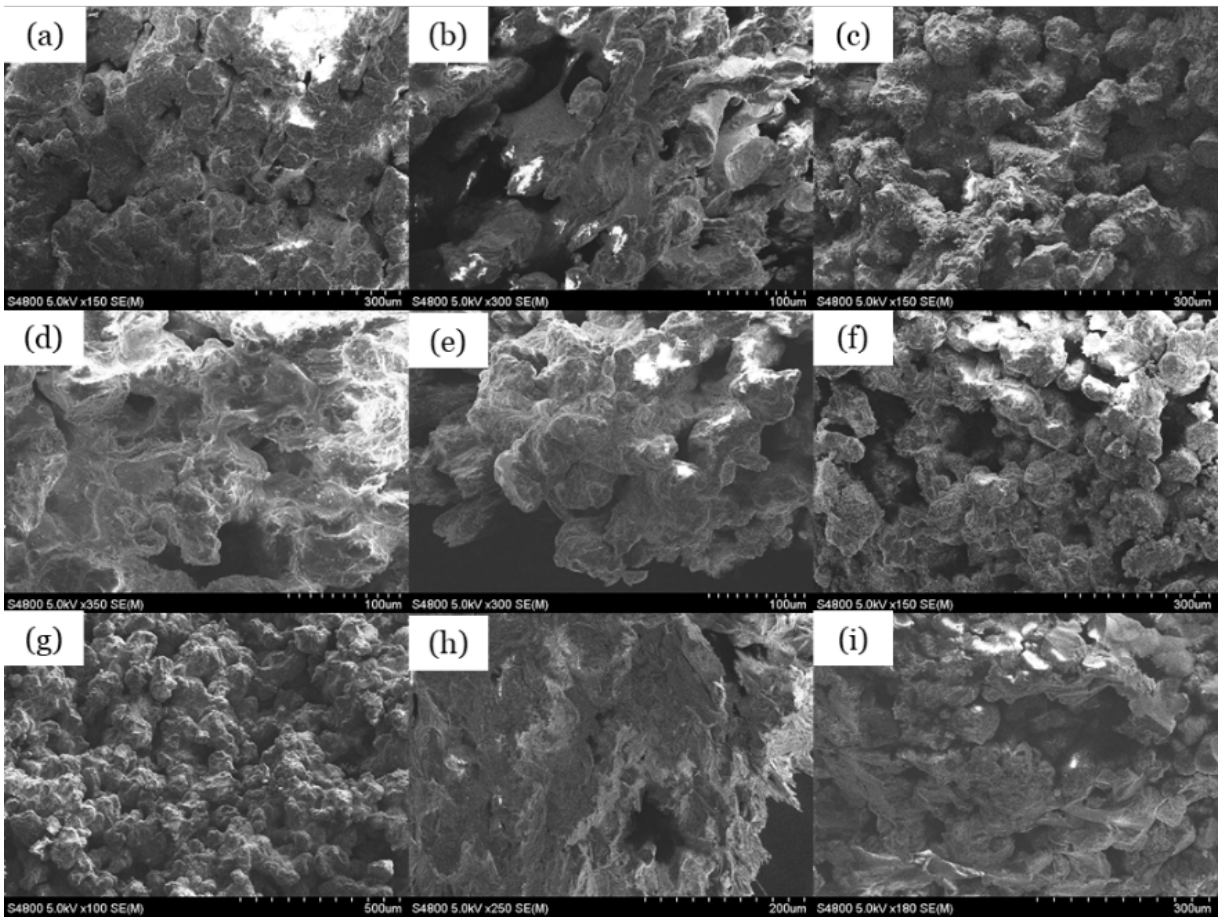

Figure 8. SEM images of (a) PA-12, (b) blend green body, (c) 111, (d) 122, (e) 211, (f) 222, (g) 312, (h) 321, and (i) 412.

Conclusion

We have demonstrated that the use of a low-melting point polymer can be used as a printing and sintering aid to fabricate high-performance polymers in desktop selective laser sintering printers. It was shown that properties of the low-melting point polymer PA-12 could be both matched and improved by a blend with its high-performance polymer counterpart PEEK despite its introduction of manufacturing disadvantages when proper heat treatments are performed. In this work, an increase of 79% in the specific mechanical properties of the printed and heat-treated polymer blend when compared to the pristine low-melting point polymer. This is believed to be caused by polymer blending as a function of the atmosphere and sintering temperatures. These results were further validated by the disappearance of the thermogravimetric peak related to the low-melting point polymer in samples where this material remained present. These results were further validated using SEM characterization, where homogeneous morphologies were observed for the polymer blend samples with the highest mechanical properties. The reported methodology can create many new research opportunities for SLS as it can be employed for virtually any other high-performance polymer using a low-temperature SLS printer with the correct selection of a matrix polymer and optimized thermal postprocessing.

Acknowledgments

This research was funded by the Department of Energy through grants DE-FE-0027502 and DE-NA0003865. The Department of Energy's Kansas City Security Campus is operated and managed by Honeywell Federal Manufacturing and Technologies, LLC under contract number DE-NA0002839. Their financial support is greatly appreciated.

References

[1] J. C. Najmon, S. Raeisi, and A. Tovar, "Review of additive manufacturing technologies and applications in the aerospace industry," in *Additive Manufacturing for the Aerospace Industry*, Elsevier, 2019, pp. 7–31.

[2] T. D. Ngo, A. Kashani, G. Imbalzano, K. T. Q. Nguyen, and D. Hui, "Additive manufacturing (3D printing): A review of materials, methods, applications and challenges," *Composites Part B: Engineering*, vol. 143. Elsevier Ltd, pp. 172–196, Jun. 15, 2018, doi: 10.1016/j.compositesb.2018.02.012.

[3] K. M. M. Billah, J. L. Coronel, M. C. Halbig, R. B. Wicker and D. Espalin, "Electrical and Thermal Characterization of 3D Printed Thermoplastic Parts With Embedded Wires for High Current-Carrying Applications," in *IEEE Access*, vol. 7, pp. 18799-18810, 2019, doi: 10.1109/ACCESS.2019.2895620.

[4] G. M. Vasquez, C. E. Majewski, B. Haworth, and N. Hopkinson, "A targeted material selection process for polymers in laser sintering," *Additive Manufacturing*, vol. 1, pp. 127–138, Oct. 2014, doi: 10.1016/j.addma.2014.09.003.

[5] D. L. Bourell, T. J. Watt, D. K. Leigh, and B. Fulcher, "Performance limitations in polymer laser sintering," in *Physics Procedia*, Jan. 2014, vol. 56, no. C, pp. 147–156, doi: 10.1016/j.phpro.2014.08.157.

[6] "The Limits of 3D Printing." https://hbr.org/2015/06/the-limits-of-3d-printing (accessed Jun. 24, 2020).

[7] P. K. Gokuldoss, S. Kolla, and J. Eckert, "Additive Manufacturing Processes: Selective Laser Melting, Electron Beam Melting and Binder Jetting—Selection Guidelines," *Materials*, vol. 10, no. 6, p. 672, Jun. 2017, doi: 10.3390/ma10060672.

[8] A. C. de Leon, Q. Chen, N. B. Palaganas, J. O. Palaganas, J. Manapat, and R. C. Advincula, "High performance polymer nanocomposites for additive manufacturing applications," *Reactive and Functional Polymers*, vol. 103. Elsevier B.V., pp. 141–155, Jun. 01, 2016, doi: 10.1016/j.reactfunctpolym.2016.04.010.

[9] T. E. Attwood, P. C. Dawson, J. L. Freeman, L. R. J. Hoy, J. B. Rose, and P. A. Staniland, "Synthesis and properties of polyaryletherketones," *Polymer*, vol. 22, no. 8, pp. 1096–1103, Aug. 1981, doi: 10.1016/0032-3861(81)90299-8.

[10] I. V. Panayotov, V. Orti, F. Cuisinier, and J. Yachouh, "Polyetheretherketone (PEEK) for medical applications," *Journal of Materials Science: Materials in Medicine*, vol. 27, no. 7. Springer New York LLC, pp. 1–11, Jul. 01, 2016, doi: 10.1007/s10856-016-5731-4.

[11] D. J. Kelsey, G. S. Springer, and S. B. Goodman, "Composite Implant for Bone Replacement," *Journal of Composite Materials*, vol. 31, no. 16, pp. 1593–1632, Aug. 1997, doi: 10.1177/002199839703101603.

[12] A. Wang, R. Lin, C. Stark, and J. H. Dumbleton, "Suitability and limitations of carbon fiber reinforced PEEK composites as bearing surfaces for total joint replacements," *Wear*, vol. 225–229, no. PART II, pp. 724–727, Apr. 1999, doi: 10.1016/S0043-1648(99)00026-5.

[13] M. Yuan, J. A. Galloway, R. J. Hoffman, and S. Bhatt, "Influence of molecular weight on rheological, thermal, and mechanical properties of PEEK," *Polymer Engineering & Science*, vol. 51, no. 1, pp. 94–102, Jan. 2011, doi: 10.1002/pen.21785.

[14] J. Devaux *et al.*, "On the molecular weight determination of a poly(aryl-ether-ether-ketone) (PEEK)," *Polymer*, vol. 26, no. 13, pp. 1994–2000, Dec. 1985, doi: 10.1016/0032-3861(85)90179-X.

[15] "PEEK Biomaterials Handbook - 2nd Edition." https://www.elsevier.com/books/peek-biomaterials-handbook/kurtz/978-0-12-812524-3 (accessed Jun. 24, 2020).

[16] "Plastics in Medical Devices - 2nd Edition." https://www.elsevier.com/books/plastics-in-medical-devices/sastri/978-1-4557-3201-2 (accessed Jun. 24, 2020).

[17] A. P. da Costa, E. C. Botelho, M. L. Costa, N. E. Narita, and J. R. Tarpani, "A review of welding technologies for thermoplastic composites in aerospace applications," *Journal of Aerospace Technology and Management*, vol. 4, no. 3. Departamento de Ciência e Tecnologia Aeroespacial, pp. 255–265, Sep. 2012, doi: 10.5028/jatm.2012.04033912.

[18] E. Resource Efficiency GmbH, "VESTAKEEP® PEEK - Processing guidelines." Accessed: Jun. 24, 2020. [Online].

[19] R. Izamshah, N. Husna, M. Hadzley, M. Amran, M. Shahir, and M. Amri, "Effects of cutter geometrical features on machining polyetheretherketones (PEEK) engineering plastic," *Journal of Mechanical Engineering and Sciences*, vol. 6, pp. 863–872, Jun. 2014, doi: 10.15282/jmes.6.2014.12.0082.

[20] S. Berretta, K. E. Evans, and O. Ghita, "Processability of PEEK, a new polymer for high temperature laser sintering (HT-LS)," *European Polymer Journal*, vol. 68, pp. 243–266, Jul. 2015, doi: 10.1016/j.eurpolymj.2015.04.003.

[21] D.-H. Lee, J.-Y. Joo, and S.-K. Lee, "Modeling of reflection-type laser-driven white lighting considering phosphor particles and surface topography," *Opt. Express, OE*, vol. 23, no. 15, pp. 18872–18887, Jul. 2015, doi: 10.1364/OE.23.018872.

[22] Alvaredo, Á., Martín, M. I., Castell, P., Guzmán de Villoria, R., & Fernández-Blázquez, J. P. (2019). Non-isothermal crystallization behavior of PEEK/Graphene nanoplatelets composites from melt and glass states. Polymers, 11(1), 124.

[23] Talbott, M. F., Springer, G. S., & Berglund, L. A. (1987). The effects of crystallinity on the mechanical properties of PEEK polymer and graphite fiber reinforced PEEK. Journal of Composite Materials, 21(11), 1056-1081.

[24] Crevecoeur, G., & Groeninckx, G. (1991). Binary blends of poly (ether ether ketone) and poly (ether imide): miscibility, crystallization behavior and semicrystalline morphology. Macromolecules, 24(5), 1190-1195.

[25] Ellis, T. S. (1995). Miscibility of polyamide blends: effects of configuration. Polymer, 36(20), 3919-3926.

[26] Schultz, J. P., Martin, J. P., Kander, R. G., & Suchicital, C. T. (2000). Selective laser sintering of nylon 12-PEEK blends formed by cryogenic mechanical alloying. In 2000 International Solid Freeform Fabrication Symposium.

[27] T. S. Ellis, "Mixing relationships in aliphatic polyamide blends," *Polymer*, vol. 33, no. 7, pp. 1469–1476, Jan. 1992, doi: 10.1016/0032-3861(92)90124-F.

[28] L. Cafiero, S. Iannace, and L. Sorrentino, "Microcellular foams from high performance miscible blends based on PEEK and PEI," *European Polymer Journal*, vol. 78, pp. 116–128, May 2016, doi: 10.1016/j.eurpolymj.2016.03.014.

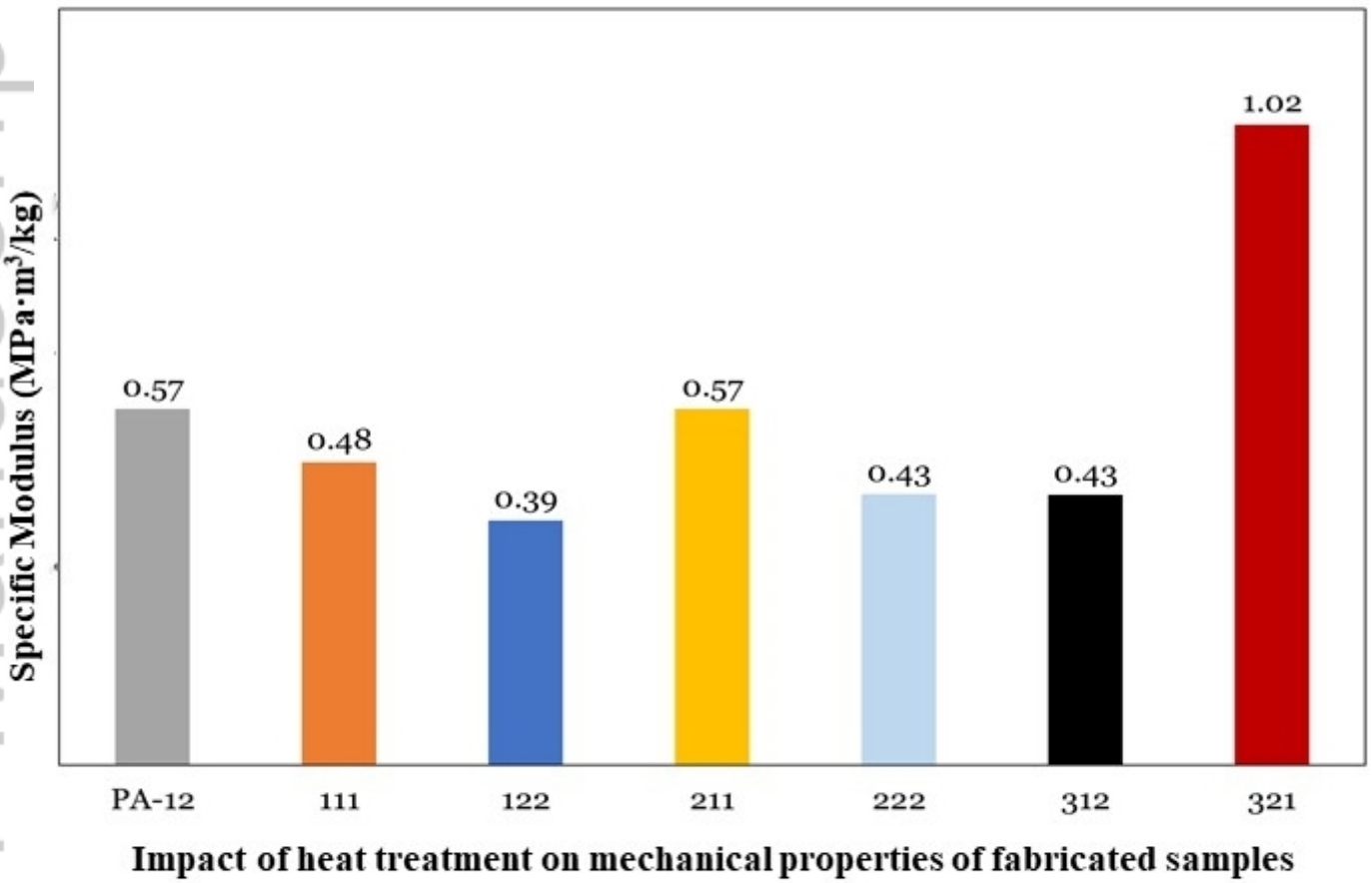

APP_52290_Graphical abstract (PEEK)1.jpg